Journal of Volcanology and Geothermal Research xxx (2009) xxx–xxx

Contents lists available at ScienceDirect

Journal of Volcanology and Geothermal Research

journal homepage: www.elsevier.com/locate/jvolgeores

Perils of petrotectonic modeling: A view from southern Sonora, Mexico

Christy B. Till *, Phillip B. Gans, Frank J. Spera, Ian MacMillan [1], Karen D. Blair [2]

Department of Earth Science, University of California, Santa Barbara, CA 93106, United States

ARTICLE INFO

Article history:
Received 12 February 2009
Accepted 30 June 2009
Available online xxxx

Keywords:
petrotectonic models
Sonora, Mexico
Gulf of California
subduction
oblique extension
pre-eruptive water content

ABSTRACT

We present major and trace element geochemical data from well-dated Oligocene–Miocene volcanic sections in southern Sonora, Mexico (28°, 110°) that span the transition from subduction to oblique extension in the proto-Gulf of California. The region of northwest Mexico including Sonora experienced this abrupt change in tectonic setting ca. 15–12.5 Ma. Syn- and post-subduction calc-alkaline volcanic rocks erupted in Sonora all have similar major and trace element signatures indicative of a continental arc setting. Post-subduction rocks in Sonora document only a subtle change in the behavior of high field strength, large ion lithophile and rare earth elements and a decrease in pre-eruptive water-content. The protracted geochemical changes in Sonora suggest it took at least 4 m.y. to erase the subduction signature from the sub-arc mantle here. Therefore Sonoran geochemistry is not consistent with the predictions of petrotectonic models and contrasts with central and southern Baja where a rapid and distinct change in the composition of lavas erupted is reported synchronous with the tectonic transition. This study exemplifies the need for caution when interpreting geochemical data for tectonic information in the absence of plate reconstructions.

1. Introduction

The use of petrochemistry to identify the tectonic setting in which magmas were formed can be traced back to the work of Marshall (1912) and Daly (1933) or in the modern era to the work of Chayes (1964) and Pearce and Cann (1971, 1973). These authors demonstrated that the trace element concentrations of basalts varied with known tectonic settings and could be used to identify paleotectonic environments. However, Pearce and Cann acknowledged the need for greater understanding of trace element partitioning and how it might have changed during Earth's history. Since the 1970's our understanding of trace element partitioning between liquids and solids of varying composition and during crystallization and melting processes has increased dramatically. Because of these scientific advances, trace elements concentrations continue to be useful petrotectonic indicators (e.g., Weigand et al., 2002; Kovács and Szabó, 2008), especially where tectonic plate reconstructions are not accessible.

Extensive work on the character of primary subduction zone lavas generated by hydrous melting of the mantle wedge demonstrates they are on average basaltic–andesitic and have trace element signatures enriched in large ion lithophile elements (LILE) and depleted in high field strength elements (HFSE) (Perfit et al., 1980; Gill, 1981; Arculus and Johnson, 1981; Dupuy et al., 1982; Pearce and Peate, 1995). Continental extension-related magmatism, generated by decompression melting of the anhydrous asthenosphere, has a greater variability in composition. Primary melts are in general similar to ocean island basalts (OIB) and can range from tholeiitic to alkaline olivine basalts. Extension-related magmas often erupt in bimodal basaltic and rhyolitic suites when involved in crustal anatexis (Christiansen and Lipman, 1972). Extension-related trace element signatures are distinguished from subduction-related signatures by their lack of HFSE depletion. Therefore petrotectonic models would predict a corresponding change in the geochemistry of the lavas, from high to low LILE /HFSE ratios, for a region that experiences a change in tectonic setting from subduction to extension.

The Gulf Extensional Province (GEP) (Gastil et al., 1975) of northwestern Mexico is a structural province defined as the region of extended continental crust in eastern Baja California, and the northwestern part of mainland Mexico adjacent to the Gulf of California (Stock and Hodges, 1989). An extensive suite of volcanic rocks was erupted within the GEP spanning the tectonic transition from subduction to oblique extension along this portion of the North American plate margin (Gastil et al., 1979; Hausback, 1984; Oskin and Stock, 2003; Mora-Klepeis and McDowell, 2004). This suite of volcanic rocks, in conjunction with the well understood plate reconstructions for this region (Atwater, 1970; Atwater, 1989; Lonsdale, 1991, 2006), make it an ideal location for determining if the geochemical response to a change in tectonic setting from subduction to extension is similar to that expected according to simple petrotectonic models. Many geochemical surveys of syn- and post-subduction volcanism on the rifted Baja peninsula have examined how the western segment of the GEP responded to the change in tectonic setting. Similar to petrotectonic predictions, a systematic change from typical arc-related calc-alkaline volcanism to a diverse

* Corresponding author. Now at Department of Earth, Atmospheric and Planetary Sciences, Massachusetts Institute of Technology, Cambridge, MA, 02139, United States.
E-mail address: ctill@mit.edu (C.B. Till).
[1] Now at Questa Environmental Consulting, Los Angeles, CA 90027, United States.
[2] Department of Physical Sciences, Houston Community College Southwest Stafford TX 77477, United States.

0377-0273/$ – see front matter © 2009 Elsevier B.V. All rights reserved.
doi:10.1016/j.jvolgeores.2009.06.014

suite of alkalic, tholeiitic, and high-Nb basaltic volcanism, in addition to local adakite volcanism, is reported for central and southern Baja, coincident with the change in tectonic setting from subduction to rifting ca. 12.5 Ma (Gastil et al., 1979; Hausback, 1984; Sawlan and Smith, 1984; Saunders et al., 1987; Bigioggero et al., 1995; Luhr et al., 1995; Negrete-Aranda and Cañón-Tapia, 2008; Castillo, 2008). However little work has been done in the eastern GEP in mainland Mexico to understand how this region of thicker continental crust (Valencio-Moreno, 2001) responded geochemically to the change in tectonic setting. Hence, this study examines a suite of volcanic rocks from the eastern GEP that offer excellent age and spatial control to test the resolution of the geochemical record in reproducing the tectonic and/or structural history of a region. Here we will show that there are only second-order changes in the major and trace element geochemistry of Sonoran volcanism during the change from subduction to extension ca. 15–12.5 Ma, which is not consistent with the predictions of petrotectonic models.

2. Tectonic and geologic background

The region of northwest Mexico now divided into the Baja peninsula and Sonora, Mexico by the Gulf of California rift, experienced subduction of the Farallon plate for most of the Tertiary. The East Pacific Rise (EPR) entered the North American trench near the latitude of present-day Los Angeles at ~25 Ma, creating the strike–slip boundary between the North American and Pacific plates (Atwater, 1970; Stock and Hodges, 1989). Continued subduction of the EPR caused this strike–slip boundary to grow in length and the cessation of the subduction zone west of Baja and Sonora to migrate south from 25–15 Ma (Dickinson and Snyder, 1979). Subduction of the EPR ceased west of Baja between 15 and 12.5 Ma, triggering the southward jump of the Rivera Triple Junction and the end of subduction west of Baja and Sonora (Lonsdale, 1991, 2006). Reconfiguration of the North American–Pacific plate boundary during the Miocene resulted in transfer of the Baja peninsula to the Pacific plate and a change in plate motion vectors from convergence to oblique divergence between 12.5 and ~6 Ma.

Magmatism related to subduction of the Farallon plate occurred in Baja California and Sonora, Mexico from 100 to 45 Ma, followed by widespread silicic magmatism in the Sierra Madre Occidental from 37 to 23 Ma (McDowell and Clabaugh, 1979). Magmatism evidently swept westward through central and western Sonora to eastern Baja from 26 to ~12 Ma, as it became more intermediate to mafic in composition (Sawlan, 1991; Aranda-Gomez and McDowell, 1998; Gans et al., 2006). This syn-subduction volcanism in Sonora was diverse and diffuse, unlike a more linear Andean-type arc. Post-subduction volcanism consisted of basaltic to rhyolitic volcanism, which persisted in coastal Sonora until ~8 Ma and on Baja and Isla Tiburon until ~6 Ma, synchronous with proto-Gulf deformation (Gastil et al., 1999; Oskin and Stock, 2003; Gans et al., 2006).

Eastern Sonora records an episodic history of Eocene to mid-Miocene volcanism, volcaniclastic sedimentation, and extensional faulting, virtually all of which predates the tectonic transition from subduction to oblique divergence (Gans, 1997; McDowell et al., 1997; Wong and Gans, 2003; Gans et al., 2006; Wong and Gans, 2008) (Fig. 1). Extension in eastern Sonora is therefore mainly "intra-arc" or "back-arc." The younger part of the volcanic record in eastern Sonora (~22–15 Ma) overlaps in age with the oldest volcanism in coastal Sonora, which facilitates a comparison of syn-subduction volcanism in an E–W transect across Sonora. Coastal Sonora is characterized by multiple NNW–SSE trending fault-bounded ranges that expose thick (>1 km) Miocene volcanic sequences erupted both syn- and post-subduction (Fig. 1). There is a conspicuous absence of volcanism in all of southern Sonora between approximately 15 and 12.5 Ma. This period of volcanic quiescence is coincident with the cessation of subduction west of Baja based on plate reconstructions from geomagnetic data. A more thorough discussion of the geology, structure, geochronology and sedimentology of these regions of Sonora can be found in associated studies (Gans, 1997; Blair and Gans, 2003; MacMillan et al., 2003; Wong and Gans, 2003; Blair and Gans, 2005; Herman and Gans, 2005; MacMillan et al., 2005; Gans et al., 2006; Wong and Gans, 2008).

3. Methods

Because of the large geographic area covered by this geochemical survey, our approach was to focus on regions where key ages of volcanism were well represented, such as coastal Sonora, rather than to equally sample all volcanic units in an E–W transect across southern Sonora. Sampling is biased toward more mafic units within all regions, as these are less likely to be affected by significant crustal contamination and crystal fractionation and more apt to reflect their source composition. 108 major-oxide and 120 trace element analyses were measured using X-ray fluorescence (XRF) and inductively coupled plasma mass spectrometry (ICP-MS), respectively, at Washington State University (Table 1; Suppl. Table S1). The $^{40}Ar/^{39}Ar$ geochronology was completed at University of California, Santa Barbara and electron microprobe analyses of phenocryst compositions were conducted on the Jeol 733 Superprobe at the Massachusetts Institute of Technology. 74 geochemical samples have been dated directly and the remaining 46 samples have well-constrained ages based on their stratigraphic position and correlation with dated sections (Table 1). These dates represent only a subset of the geochronology of these regions, as they bear directly on the geochemical interpretation. Geologic mapping and detailed geochronology of the individual regions within the study area will be presented elsewhere. The period of volcanic quiescence between 15 and 12.5 Ma was punctuated by the eruption of two volumetrically insignificant lava flows in southern Sonora, a dacite in Sierra Mazatan at 14.21 Ma and a basalt in Sierra Libre at 13.0 Ma (Mora-Klepeis and McDowell, 2004; Gans et al., 2006). The dacite has a trace element signature characteristic of subduction-related volcanism, while the basalt does not. We therefore, chose 14 Ma as the division between syn- and post-subduction samples for comparison of major and trace element compositions, although the entire period between 15 and 12.5 Ma is thought by the authors to represent the timing of subduction cessation at the latitude of this study based on plate reconstructions.

4. Geochemical results

Whole rock compositions range from calc-alkaline basalt to rhyolite with no distinct changes after subduction ceased (Table 1; Fig. 2). Samples older than 14 Ma exhibit a more homogeneous range of compositions (49–67% SiO_2) in part due to our sampling bias toward more mafic volcanic rocks. Six andesite samples between 21 and 10 Ma have characteristics of high Mg# andesites ($(Mg/Mg+Fe)\times 100 > 0.45$ and 54–65 wt.% SiO_2: Kelemen et al., 2003).

MORB-normalized trace element plots of all andesites (53 samples) and basalts (20 samples) exhibit a typical continental arc signature with the characteristic enrichment in LILE and depletion in HFSE. Both the andesites and basalts have persistent arc-like trace element signatures after subduction ceases (ca. 14 Ma). Detailed examination of these signatures reveals the subduction-related LILE-enrichments, for example Rb and Th in the basalts, do decrease from ~14 Ma until volcanism ceased at ~8 Ma (Fig. 3; Suppl. Table S1). Similar to the change in LILE and HFSE, the rare earth elements (REE) patterns of the basalts become progressively less fractionated after subduction ceases (Fig. 4). These subtle changes in trace element behavior can be further quantified with trace element ratios. Ba/Ta is apt to reflect a fluid component from subducted oceanic crust and/or sediments due to the solubility of Ba in aqueous fluids relative to Ta (Spera et al., 2007). Ba/Ta values are similar during and after

Please cite this article as: Till, C.B., et al., Perils of petrotectonic modeling: A view from southern Sonora, Mexico, J. Volcanol. Geotherm. Res. (2009), doi:10.1016/j.jvolgeores.2009.06.014

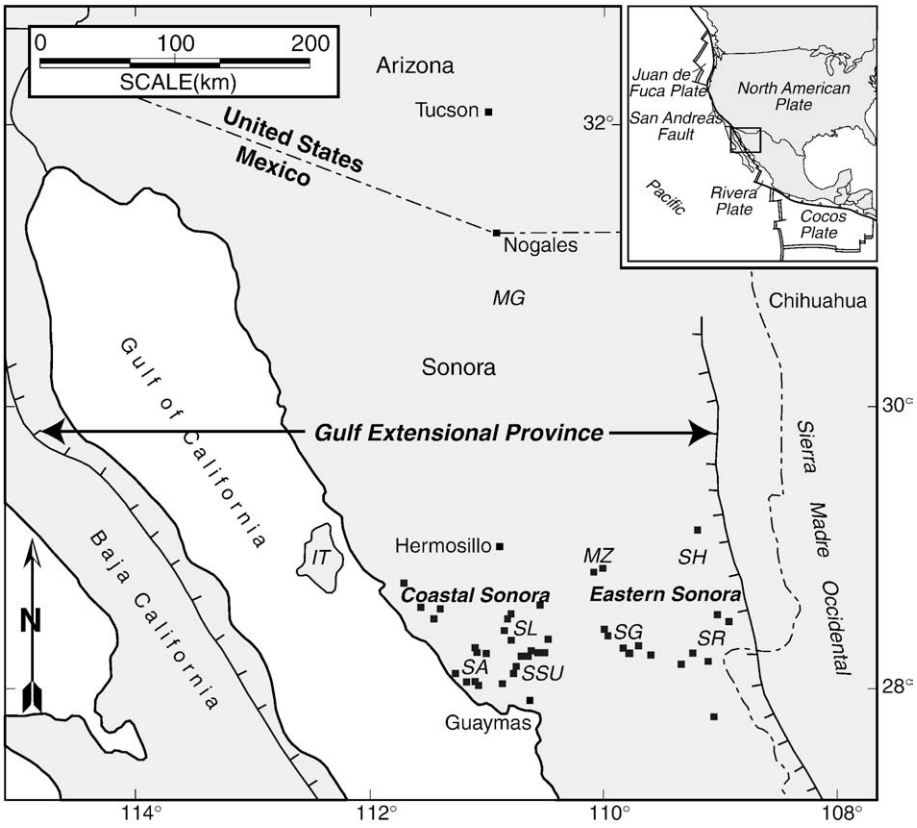

Fig. 1. Map of the Gulf Extensional Province and Sonora. Regions sampled in this study: Sahuaripa (SH), Santa Rosa (SR), Suaqui Grande (SG), Sierra Mazatan (MZ), Sierra Santa Ursula (SSU), Sierra Libre (SL), Sierra El Aguaje (SA), and Guaymas. Also identified are Isla Tiburon (IT) and the Magdalena metamorphic core complex (MG). Modified from Gans (1997).

subduction, although the maximum Ba/Ta values decrease substantially after subduction ceases (Fig. 4). Dy/Yb ratios, which reflect the fractionation of the middle and heavy REE, are also similar before and after subduction but exhibit a decrease in maximum values after subduction ceased (Fig. 4).

An independent method to identify differences between syn- and post-subduction lavas is to evaluate their water content. We calculate the pre-eruptive H_2O-content of Sonoran lavas by simultaneous solution of the olivine-liquid geothermometer and olivine–clinopyroxene–plagioclase hygrometer of Sisson and Grove (1993). If syn-subduction lavas are indeed the product of hydrous melting of the mantle wedge during subduction, as indicated by their continental arc trace element signatures, we expect them to have relatively high water contents (>4 wt.%). If post-subduction lavas are the product of anhydrous decompression melting of asthenospheric mantle, then we expect them to be relatively water-poor. Alternately, if post-subduction lavas are the product of decompression melting or conductively reheating mantle lithosphere previously modified by subduction-related fluid or melt, we might expect them to exhibit intermediate to low water contents (2–4 wt.%) due to the breakdown of residual hydrous phases such as amphibole or phlogopite. Six mafic samples (Mg#>0.5) ranging in age from 26.4 to 8.9 Ma multiply saturated with olivine, clinopyroxene, and plagioclase were first chosen as a sample set. The composition of the olivine phenocrysts were determined by electron microprobe and used in conjunction with the whole rock major and trace element analyses for thermometric and hygrometric calculations (Suppl. Table S2). For the calculations, we assume a pressure of 1 GPa and that whole rock compositions approximate liquid compositions. We find a good correlation ($R^2=0.97$) between the calculated pre-eruptive H_2O-content and temperature of crystallization. The six test samples range in pre-eruptive H_2O-content from 0.50 to 2.50 wt.% H_2O (Fig. 5). This method was then applied to the 71 most mafic samples from Sonora that range in age from 28.3 to 8.9 Ma and for which the composition of the liquidus olivine was calculated assuming $K_D^{Fe-Mg}=0.29$ as in Sisson and Grove (1993). These 71 samples also demonstrate a good correlation ($R^2=0.95$) between the calculated pre-eruptive H_2O-content and temperature of crystallization. Samples erupted during subduction (28.3–15 Ma) vary from 0 to 7.9 wt.% H_2O (Fig. 5a). Samples erupted after 12.5 Ma show a decline from 5.4 to 0 wt.% H_2O over 3.5 m.y. When pre-eruptive H_2O-content is plotted against longitude, it is evident all the driest samples (<2 wt.% H_2O) erupted in the coastal region of Sonora (Fig. 5b).

5. Discussion

27–8 Ma mafic volcanic rocks erupted in southern Sonora overall have typical arc signatures but reveal subtle changes in their trace element concentrations after subduction ceases as demonstrated by their spider patterns and trace element ratios. There is a distinct decrease in the maximum value of chemical subduction indicators, such as H_2O-content, Ba/Ta, Dy/Yb, and Rb-content, when subduction ceases for individual samples as well as the entire suite of mafic samples (Figs. 4a, b and 5a). The simplest interpretation of these observations and calculations is that the trace element abundances and H_2O-contents represent the abundance of metasomatized (slab fluid- or melt-modified) peridotite in the mantle at the time each melt was formed. Minimum Nb and Ta values are similar to average MORB values and therefore consistent with models attributing arc signatures to the preferential enrichment and depletion of the LILE and HFSE, respectively, in the mantle wedge by the addition of slab fluids or melts. Work on Mt. Shasta andesites by Grove et al. (2002) suggests LREE enrichments and Dy/Yb concentrations in rocks similar to Sonoran syn-subduction andesites and basalts can be attributed to a subduction-related fluid-rich component in the melting region. Therefore the change over time in LREE, trace element ratios, and

Please cite this article as: Till, C.B., et al., Perils of petrotectonic modeling: A view from southern Sonora, Mexico, J. Volcanol. Geotherm. Res. (2009), doi:10.1016/j.jvolgeores.2009.06.014

Table 1
Major element geochemistry, age and location of all samples in this study. Errors on $^{40}Ar/^{39}Ar$ ages are 2σ. Ages in parenthesis are inferred based on stratigraphic position. XRF major oxide chemistry is normalized to 100%.

Sample ID	XRF	ICPMS	SiO2	TiO2	Al2O3	FeO	MnO	MgO	CaO	Na2O	K2O	P2O5	Total	$^{40}Ar/^{39}Ar$ age	Reference	Easting (UTM)	Northing (UTM)
Santa Rosa																	
95SN-1	*	*	60.13	0.955	17.15	6	0.106	2.81	6.15	3.79	2.51	0.403	99.61	17.45 ± 0.10 Ma	1	670410	3148360
95SR-11	*	*	54.57	1.309	17.73	8.34	0.138	3.72	8.09	3.53	1.94	0.628	99.19	26.40 ± 0.50 Ma	1	680300	3157850
95SR-56		*	–	–	–	–	–	–	–	–	–	–	–	22.60 ± 0.30 Ma	1	680450	3159425
95SR-72	*	*	54.29	1.284	17.51	8.34	0.138	4.6	8.02	3.39	1.82	0.613	99.19	26.40 ± 0.50 Ma	1	682675	3157650
95SR-101	*	*	56.12	1.223	17.12	7.45	0.116	4.48	7.04	3.67	2.31	0.48	98.97	18.00 ± 0.40 Ma	1	669890	3134325
Suaqui Grande																	
96SN-010	*	*	63.89	0.684	15.93	4.97	0.092	2.77	5.06	3.18	3.3	0.134	100	61.58 ± 0.32 Ma	2	633680	3133840
96SN-019	*	*	70.41	0.383	15.18	2.67	0.038	1.18	2.32	3.61	4.05	0.154	100	26.34 ± 0.22 Ma	2	614050	3138599
96SN-32		*	–	–	–	–	–	–	–	–	–	–	–	27.60 ± 0.40 Ma	2	643460	3142759
96SN-33	*	*	52.04	1.533	18.69	8.81	0.124	3.84	8.8	3.73	1.67	0.777	100	25.93 ± 0.06 Ma	2	643410	3143838
96SN-046	*	*	67.12	0.498	15.61	3.9	0.061	1.88	4	3.35	3.47	0.119	100	59.27 ± 0.30 Ma	2	633120	3157250
96SN-060	*	*	56.19	0.919	18.93	7.1	0.105	3.02	7.01	4.1	2.15	0.469	100	21.40 ± 1.60 Ma	2	627070	3146997
96SN-73		*	–	–	–	–	–	–	–	–	–	–	–	25.84 ± 0.14 Ma	2	618430	3152598
96SN-076	*	*	78.55	0.117	11.53	1.51	0.041	0.31	1.73	2.11	4.08	0.017	100	12.41 ± 0.06 Ma	2	617000	3126499
96SN-077	*	*	75.92	0.236	13.77	1.53	0.05	1.51	4	0.63	2.29	0.06	100	24.45 ± 0.10 Ma	2	616260	3126818
96SN-82		*	–	–	–	–	–	–	–	–	–	–	–	25.81 ± 0.12 Ma	2	612820	3143729
96SN-088	*	*	57.1	0.73	19.32	7.08	0.083	2.02	7	3.97	2.3	0.399	100	27.30 ± 1.00 Ma	2	611990	3150460
96SN-106	*	*	52.06	1.784	17.99	9.95	0.146	3.44	8.09	3.84	2	0.698	100.06	25.60 ± 0.60 Ma	2	608340	3159640
96SN-131		*	–	–	–	–	–	–	–	–	–	–	–	20.59 ± 0.10 Ma	2	638620	3144360
96SN-137		*	–	–	–	–	–	–	–	–	–	–	–	26.3 ± 0.40 Ma	2	636610	3143700
96SN-145		*	–	–	–	–	–	–	–	–	–	–	–	25.66 ± 0.14 Ma	2	638900	3146160
96SN-147	*	*	52.68	1.605	17.37	9.18	0.148	4.37	8.9	3.53	1.77	0.449	99.41	20.65 ± 0.08 Ma	2	635950	3146200
Sahuaripa																	
02KBS-013	*	*	57.65	1.043	18.13	6.08	0.09	2.27	7.09	4.07	3.01	0.556	100	15.2 ± 0.10 Ma	3	672268	3196317
02KBS-017	*	*	51.76	2.136	16.92	10.43	0.148	4.33	7.95	3.77	1.69	0.878	100	24.87 ± 0.10 Ma	3	673548	3219510
02KBS-029	*	*	50.75	1.978	16.9	10.11	0.102	4.68	9.63	3.57	1.46	0.825	100	28.30 ± 1.0 Ma	3	667798	3229433
02KBS-030	*	*	61.36	0.757	17.82	4.9	0.096	2.61	5.77	3.91	2.5	0.276	100	16.16 ± 0.18 Ma	3	673001	3189776
02KBS-035	*	*	50.98	2.139	17.43	9.36	0.142	4.46	9.32	3.45	1.39	1.326	100	27.53 ± 0.1 Ma	3	680651	3200177
02KBS-038	*	*	62.48	0.711	17.4	4.65	0.094	2.2	5.72	3.79	2.74	0.219	100	15.92 ± 0.06 Ma	3	676987	3187455
02KBS-043	*	*	52.93	1.612	18.88	8.47	0.167	3.61	8.03	3.61	2.21	0.495	100	27.34 ± 0.08 Ma	3	680652	3204841
03KBS-57	*	*	53.44	1.683	17.24	9.51	0.122	3.53	8.06	3.43	2.19	0.794	99.32	25.90 ± 0.20 Ma	3	669719	3227601
03KBS-059	*	*	50.92	2.326	16.85	9.54	0.209	4.71	8.83	3.66	1.64	1.32	100	27.68 ± 0.10 Ma	3	673626	3216012
03KBS-081	*	*	47.93	2.254	16.42	11.05	0.184	7.43	9.64	3.54	1.04	0.517	100	19.12 ± 1.0 Ma	3	679823	3180368
Sierra Libre																	
04CTSL-002	*	*	47.57	1.291	17.54	9.05	0.15	8.69	12.44	2.94	0.23	0.115	99.33	(~13.0 Ma)	4	508984	3171898
02IMSL-01	*	*	75.44	0.147	12.53	1.93	0.027	0.03	0.22	3.35	6.32	0.02	99.32	12.34 ± 0.04 Ma	4	497280	3151172
02IMSL-02	*	*	61.81	0.746	16.98	5.25	0.065	2.78	5.73	3.88	2.54	0.225	98.9	(~11.9 Ma)	4	495805	3150393
02IMSL-03	*	*	51.45	1.567	16.83	10.61	0.149	5.7	9.42	3.25	0.87	0.157	98.34	13.0 ± 0.3 Ma	4	496106	3150481
02IMSL-04	*	*	59.15	1.913	14.98	8.72	0.163	2.44	5.25	4.42	2.47	0.49	99.52	(12.2–11.1 Ma)	4	496221	3150460
H-IMSL-6A	*	*	65.47	1.178	14.82	5.92	0.131	1.06	3.33	4.3	3.45	0.343	99	(12.2–11.1 Ma)	4		
02IMSL-09	*	*	75.62	0.148	12.44	2	0.034	0	0.55	3.53	5.67	0.011	97.49	(12.2–11.1 Ma)	4	499617	3150499
H-IMSL-11	*	*	67.55	0.482	14.09	6.66	0.164	0.01	0.88	5.17	4.93	0.074	97.96	(12.2–11.1 Ma)	4		
H-IMSL-12	*	*	75.61	0.172	12.25	2.19	0.047	0	0.7	3.43	5.59	0.013	97.02	(12.2–11.1 Ma)	4	528720`	3145447
02IMSL-13	*	*	60.9	1.322	14.77	7.18	0.127	3.25	5.91	3.41	2.86	0.271	99.4	10.26 ± 0.04 Ma	4	511297	3141602
02IMSL-15	*	*	76.7	0.154	11.88	1.95	0.036	0	0.59	3.41	5.27	0.012	97.19	12.15 ± 0.04 Ma	4	528720	3145447
02IMSL-19	*	*	58.65	1.35	16.78	6.63	0.109	3.92	6.85	4.05	1.34	0.329	99.46	(10.7–10.2 Ma)	4	492096	3146456
H-IMSL-19a	*	*	75.31	0.121	12.78	1.86	0.058	0.06	0.92	3.77	5.09	0.021	98.97	(12.2–11.1 Ma)	4		
H-IMSL-19b	*	*	75.04	0.134	13.07	1.95	0.026	0.03	0.9	3.75	5.06	0.057	98.56	(12.2–11.1 Ma)	4		
02IMSL-22	*	*	68.18	0.45	14.06	6.3	0.166	0.02	0.79	4.94	5.04	0.054	98.46	(12.2–11.1 Ma)	4	497867	3148997
H-IMSL-24	*	*	69.35	0.791	13.65	4.17	0.102	0.87	2.53	4.14	4.21	0.196	98.69	(12.2–11.1 Ma)	4		
H-IMSL-24a	*	*	62.89	1.514	14.9	7.39	0.124	1.7	4	4.18	2.94	0.383	98.57	(12.2–11.1 Ma)	4		
H-IMSL-24b	*	*	58.98	1.905	15.14	8.55	0.161	2.39	5.23	4.67	2.46	0.496	99.34	(12.2–11.1 Ma)	4		
H-IMSL-25	*	*	64.42	1.254	14.72	6.53	0.102	1.43	3.7	4.25	3.23	0.363	99.01	(12.2–11.1 Ma)	4		
H-IMSL-28	*	*	75.86	0.147	12.41	2.05	0.038	0	0.59	3.98	4.92	0.014	97.3	(12.2–11.1 Ma)	4	497932	3152649
03IMSL-29	*	*	66.44	0.532	16.06	3.73	0.07	1.87	3.88	3.96	3.24	0.21	98.29	19.5 ± 0.1 Ma	4	496600	3153832
H-IMSL-31	*	*	64.37	1.256	14.78	6.51	0.143	1.31	3.76	4.24	3.26	0.372	98.84	(12.2–11.1 Ma)	4	526832	3140499
04IMSL-31	*	*	61.41	0.741	17.41	5.01	0.078	2.22	5.83	3.89	3.08	0.323	98.77	(12.2–11.1 Ma)	4	526832	3140499
04IMSL-39	*	*	76.28	0.134	12.62	1.95	0.043	0.07	0.83	4.69	3.37	0.013	96.77	12.34 ± 0.04 Ma	4	517461	3165400
Sierra Santa Ursula																	
04CTSSU-002	*	*	57.84	0.841	17.04	6.31	0.108	4.06	6.8	3.8	2.77	0.422	97.9	(~23 Ma)	4	508737.3143	3119582.686
04CTSSU-004	*	*	56	0.874	17.77	7.15	0.122	4.73	7.1	3.81	2.12	0.323	97.67	(~23 Ma)	4	509000.1714	3120139.943
04CTSSU-005	*	*	49.27	1.535	12.94	7.99	0.14	11.47	9.85	3.48	2.23	1.101	97.87	(21.3 Ma)	4	509126.3429	3120728.743
04CTSSU-006	*	*	63.9	0.66	16.79	4.46	0.071	1.57	5.19	4.13	2.93	0.294	98.98	(~23 Ma)	4	509904.4	3120423.829
04CTSSU-007	*	*	54.16	0.77	16.83	7.38	0.128	7.29	8.66	3.46	1.15	0.167	99.26	(~20.7 Ma)	4	509862.3429	3119656.286
04CTSSU-008	*	*	48.95	1.012	14.42	8.47	0.145	11.93	9.63	2.88	2.08	0.499	98.39	(~21.3 Ma)	4	509452.2857	3120318.686
04CTSSU-009	*	*	70.86	0.407	14.54	3.26	0.069	0.41	2.24	3.86	4.26	0.094	99.16	(~11.9 Ma)	4	511176.6286	3119835.029
04CTSSU-012	*	*	56.77	0.896	16.59	7.02	0.125	4.37	7.73	3.13	3.01	0.354	99.19	(~21.6 Ma)	4	509010.6857	3122579.257
04CTSSU-013	*	*	64.03	1.191	14.72	7.35	0.113	1.03	3.01	4.1	4.04	0.424	99.04	(~12 Ma)	4	513069.2	3119656.286

Please cite this article as: Till, C.B., et al., Perils of petrotectonic modeling: A view from southern Sonora, Mexico, J. Volcanol. Geotherm. Res. (2009), doi:10.1016/j.jvolgeores.2009.06.014

Table 1 (*continued*)

Sample ID	XRF	ICPMS	SiO2	TiO2	Al2O3	FeO	MnO	MgO	CaO	Na2O	K2O	P2O5	Total	$^{40}Ar/^{39}Ar$ age	Reference	Easting (UTM)	Northing (UTM)
Sierra Santa Ursula (cont.)																	
04CTSSU-015	*	*	55.92	2.538	13.53	11.13	0.168	3	7.5	3.35	2.38	0.486	97.98	(~11.7 Ma)	4	514303.4642	3121710.179
04CTSSU-016	*	*	52.3	1.649	16.57	9.21	0.153	6.02	9.25	3.36	1.15	0.327	99.38	(~20.7 Ma)	4	517128.1786	3124631.464
04IMSU-10	*	*	56.43	0.858	17.6	6.79	0.108	4.34	7.41	3.5	2.66	0.304	98.49	21.6 ± 0.4 Ma	4	507890	3121109
04IMSU-11	*	*	54.72	0.939	16.24	7.19	0.125	7.63	7.92	3.4	1.54	0.288	99.63	(~20.7 Ma)	4	507074	3123310
04IMSU-13	*	*	58.87	0.807	17.97	6.15	0.064	2.83	6.95	3.64	2.4	0.309	98.62	(~21.6 Ma)	4	509141	3119528
04IMSU-20	*	*	58.94	0.886	17.29	5.97	0.097	2.83	6.8	4.24	2.51	0.422	98.17	(23 Ma)	4	511990	3122186
04IMSU-23	*	*	55.89	1.078	17.39	7.15	0.124	5.1	7.06	3.86	1.97	0.38	98.83	(~20.7 Ma)	4	512732	3119985
04IMSU-24	*	*	62.81	1.352	14.72	7.88	0.132	1.23	3.52	4.09	3.74	0.529	98.88	(~12 Ma)	4	512866	3119975
04IMSU-27	*	*	56.77	2.147	16.76	10.43	0.152	1.97	5.87	4.01	1.39	0.499	98.16	(~20.7 Ma)	4	519517	3123420
Sierra El Aguaje																	
02PGS-24	*	*	57.46	1.088	16.23	6.42	0.127	5.61	7.82	3.48	1.41	0.356	99.96	8.90 ± 0.20 Ma	2	482825	3130739
02PGS-25	*	*	65.92	0.661	16.66	3.64	0.07	2.06	4.81	4.45	1.55	0.187	100	9.00 ± 0.22 Ma	2	481048	3131284
02PGS-26	*	*	55.11	1.355	16.87	6.83	0.123	5.17	8.93	3.69	1.51	0.411	99.7	9.02 ± 0.06 Ma	2	485462	3131156
02PGS-28	*	*	51.21	2.12	17.19	8.94	0.154	5.82	8.75	4	1.25	0.563	100	9.12 ± 0.06 Ma	2	493655	3110851
02PGS-34	*	*	54.67	0.948	16.83	6.56	0.108	7.86	7.69	3.18	1.83	0.32	100.08	16.50 ± 0.08 Ma	2	496410	3096776
02PGS-35	*	*	54.35	2.063	16.39	9.23	0.162	4.06	7.64	3.69	1.99	0.426	98.96	10.80 ± 0.20 Ma	2	496824	3096774
02PGS-41	*	*	64.46	0.621	17.08	4.02	0.081	1.96	5.17	3.94	2.39	0.271	98.51	15.30 ± 0.12 Ma	2	488910	3095400
02PGS-42A	*	*	77.99	0.052	12.27	0.78	0.032	0	0.44	3.83	4.6	0.023	99.91	10.70 ± 0.16 Ma	2	487945	3100026
03PGS-53B	*	*	76.88	0.156	12.52	1.05	0.021	0.13	0.97	3.58	4.66	0.026	100	10.15 ± 0.06 Ma	2	496173	3110007
03PGS-54		*	–	–	–	–	–	–	–	–	–	–	–	10.13 ± 0.05 Ma	2	496200	3110134
03PGS-58	*	*	50.93	2.073	16.08	9.34	0.152	7.29	8.4	3.69	1.47	0.568	100	9.01 ± 0.04 Ma	2	495160	3109337
03PGS-62	*	*	64.07	0.614	16.73	4.89	0.099	2.51	5.15	3.33	2.47	0.143	100	10.66 ± 0.22 Ma	2	482058	3098938
03PGS-64	*	*	59.09	0.742	15.62	5.64	0.086	6.2	7.19	3.09	2.04	0.305	100.36	21.00 ± 0.15 Ma	2	485825	3100435
03PGS-67	*	*	67.33	0.591	16.21	3.27	0.061	1.65	3.91	4.06	2.75	0.168	100	8.32 ± 0.15 Ma	2	482584	3109368
03PGS-73	*	*	63.61	0.942	16.74	4.68	0.087	2.04	4.93	4.65	2.09	0.235	100	9.19 + 0.04 Ma	2	481824	3107627
03PGS-74		*	–	–	–	–	–	–	–	–	–	–	–	9.91 ± 0.06 Ma	2	482017	3104443
03PGS-75	*	*	50.98	1.905	17.13	10.05	0.138	5.73	9.26	3.65	0.87	0.289	100	10.00 ± 0.30 Ma	2	481391	3104783
04PGS-081	*	*	56.76	1.189	17.05	6.67	0.095	4.3	6.98	3.64	2.83	0.474	100	11.50 ± 0.15 Ma	2	491153	3100612
04PGS-094	*	*	60.06	1.079	17.49	6.36	0.112	2.67	5.87	3.97	2.18	0.207	100	(<12.10 Ma)	2	500341	3098786
04PGS-104	*	*	70.1	0.763	14.07	4.05	0.066	0.57	1.74	3.74	4.72	0.181	100	(~11.2–12 Ma)	2	552039	3116903
04CTSA-1	*	*	53.79	1.25	16.91	7.88	0.127	6.05	7.95	3.54	2.07	0.432	98.65	(20 or 16 Ma)	2	489521	3097494
O4CTSA-2	*	*	53.9	1.256	17.14	7.92	0.111	5.76	8.02	3.52	1.95	0.421	98.67	(20 or 16 Ma)	2	489552	3097509
04CTSA-4	*	*	56.62	0.858	17.28	7.31	0.164	4.61	7.16	3.38	2.23	0.39	98.88	(~15.7 Ma)	2	489664	3097550
04CTSA-5	*	*	58.42	0.884	16.51	6.35	0.104	5.3	6.65	3.48	1.97	0.335	98.23	(~15.7 Ma)	2	489725	3097624
04CTSA-7	*	*	52.05	1.744	17.37	9.79	0.155	4.82	8.34	3.69	1.68	0.355	98.31	(~11.9–11.3 Ma)	2	489711	3097799
04CTSA-8	*	*	55.65	1.813	16.31	9.09	0.132	3.45	6.63	4.05	2.44	0.433	99.08	(~11.9–11.3 Ma)	2	489711	3097799
04CTSA-9	*	*	51.36	1.652	17.93	9.14	0.096	5.5	9.22	3.57	1.19	0.343	98.09	(~11.9–11.3 Ma)	2	489753	3097914
04CTSA-10	*	*	51.13	2.039	17.14	9.97	0.156	5.26	8.75	3.71	1.44	0.393	98.05	(~11.9–11.3 Ma)	2	489753	3097914
SE Sonora																	
03PGS-Nuri1	*	*	54.72	1.451	17.8	7.71	0.13	3.96	6.45	4.24	2.83	0.713	100.01	16.40 ± 0.10 Ma	2	664591	3109940
Coastal Sonora																	
01PGS-35A	*	*	76.28	0.131	12.79	1.68	0.041	0.13	0.97	4.99	2.98	0.018	100	12.37 ± 0.04 Ma	2	402169	3195182
02PGS-01	*	*	76.1	0.124	12.63	1.62	0.04	0.09	0.68	4.13	4.57	0.015	100	12.25 ± 0.10 Ma	2	500758	3203873
02PGS-07	*	*	55.09	1.585	16.32	7.61	0.136	5.53	8.45	3.62	1.31	0.342	99.62	10.02 ± 0.17 Ma	2	478909	3176173
02PGS-8		*	–	–	–	–	–	–	–	–	–	–	–	10.70 ± 0.25 Ma	2	478706	3176107
02PGS-09	*	*	54.37	1.347	16.36	7.21	0.127	6.39	9.23	3.48	1.15	0.33	99.32	10.65 ± 0.06 Ma	2	476427	3169507
02PGS-12	*	*	63.04	1.318	15.64	5.57	0.108	1.98	4.74	4.05	3.21	0.342	100	11.41 ± 0.04 Ma	2	471891	3163132
02PGS-13	*	*	50.54	1.537	16.88	8.53	0.162	7.51	10.8	3.33	0.5	0.21	100	9.50 ± 0.15 Ma	2	47563	3155326
02PGS-15	*	*	51.01	1.575	16.85	8.61	0.161	7.37	10.28	3.31	0.61	0.237	100	9.00 ± 1.00 Ma	2	471831	3154577
02PGS-19		*	–	–	–	–	–	–	–	–	–	–	–	8.25 ± 0.25 Ma	2	459283	3133526
Guaymas																	
02PGS-32	*	*	56.27	0.787	16.92	6.79	0.118	7.09	7.08	3.51	1.26	0.169	100.1	17.00 ± 0.50 Ma	2	500544	3100191
03PGS-50	*	*	49.91	2.005	16.19	10.33	0.179	7.41	9.69	3.27	0.65	0.366	99.05	10.40 ± 0.10 Ma	2	531557	3091086
Sierra Mazatan																	
01PGS-02	*	*	61.08	0.762	17.18	5.24	0.092	2.86	6.03	3.83	2.65	0.274	100	24.20 ± 0.10	5	548471	3213558
02MAZ-069	*	*	76.31	0.12	12.6	1.56	0.017	0.16	0.33	3.69	5.16	0.062	100	12.44 ± 0.10 Ma	5	581811	3233061
03MAZ-83	*	*	64.08	0.671	16.71	4.08	0.089	2.25	5.33	3.88	2.68	0.23	100	14.21 ± 0.06 Ma	5	569665	3235475
03MAZ-129	*	*	56.18	1.411	18.86	3.81	0.14	1.52	8.73	4.58	3.78	1	100	16.50 ± 0.50 Ma	5	574930	3235209
03MAZ-132	*	*	58.04	1.17	17.64	6.3	0.131	1.71	6.34	4.38	3.51	0.785	100	17.86 ± 0.06 Ma	5	572770	3241435
03MAZ-078	*	*	62.49	0.759	17.08	4.82	0.087	2.4	5.48	3.83	2.78	0.28	100	15.19 ± 0.12 Ma	5	581180	3236375

References:
1=Gans, 1997.
2=Gans et al., 2006 and Gans, pers. comm., 2009.
3=Blair and Gans, 2003, 2005 and Blair, pers. comm., 2006.
4=MacMillan et al., 2003, 2005 and MacMillan, pers. comm., 2006.
5=Wong and Gans, 2003, 2008.

Please cite this article as: Till, C.B., et al., Perils of petrotectonic modeling: A view from southern Sonora, Mexico, J. Volcanol. Geotherm. Res. (2009), doi:10.1016/j.jvolgeores.2009.06.014

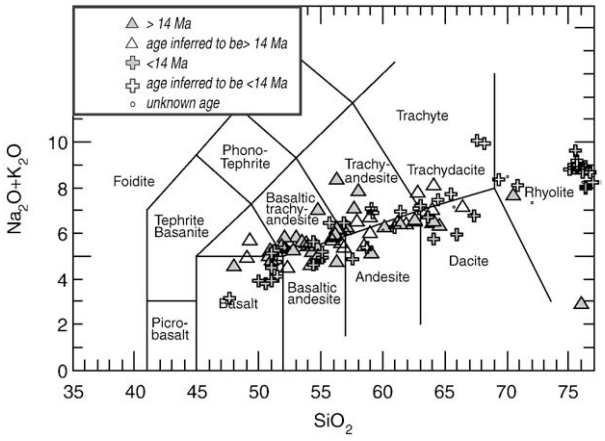

Fig. 2. Alkali-silica classification diagram (Le Bas et al., 1992) for all samples divided by age.

H_2O-contents is consistent with a decrease in the amount of metasomatized mantle in the source region once subduction ceases.

The residual arc characteristics in <14 Ma volcanism suggests the time required to completely erase the subduction signature from the sub-arc mantle was greater than the 4 million years of volcanism that post-dated subduction in Sonora. Intermediate H_2O-content (2–4 wt.%) post-subduction magmas likely formed when crustal extension in Sonora trigged conductive reheating or decompression melting of reservoirs of mantle lithosphere previously modified by subduction-related fluid or melt (Fig. 6). The high Mg # andesites erupted during subduction have arc trace element signatures and likely represent water-rich primary melts of the mantle wedge rather than melts of oceanic slab (Grove et al., 2002). Post-subduction high Mg# andesites were likely formed by the remobilization of lithosphere reservoirs of water-rich primary melts. Coastal Sonora was the focus of <12.5 Ma proto-Gulf extension and consequent melting, which likely explains the range of post-subduction H_2O-contents found here from intermediate H_2O-contents (2–4 wt.%) to the minimum values observed (<1 wt.%).

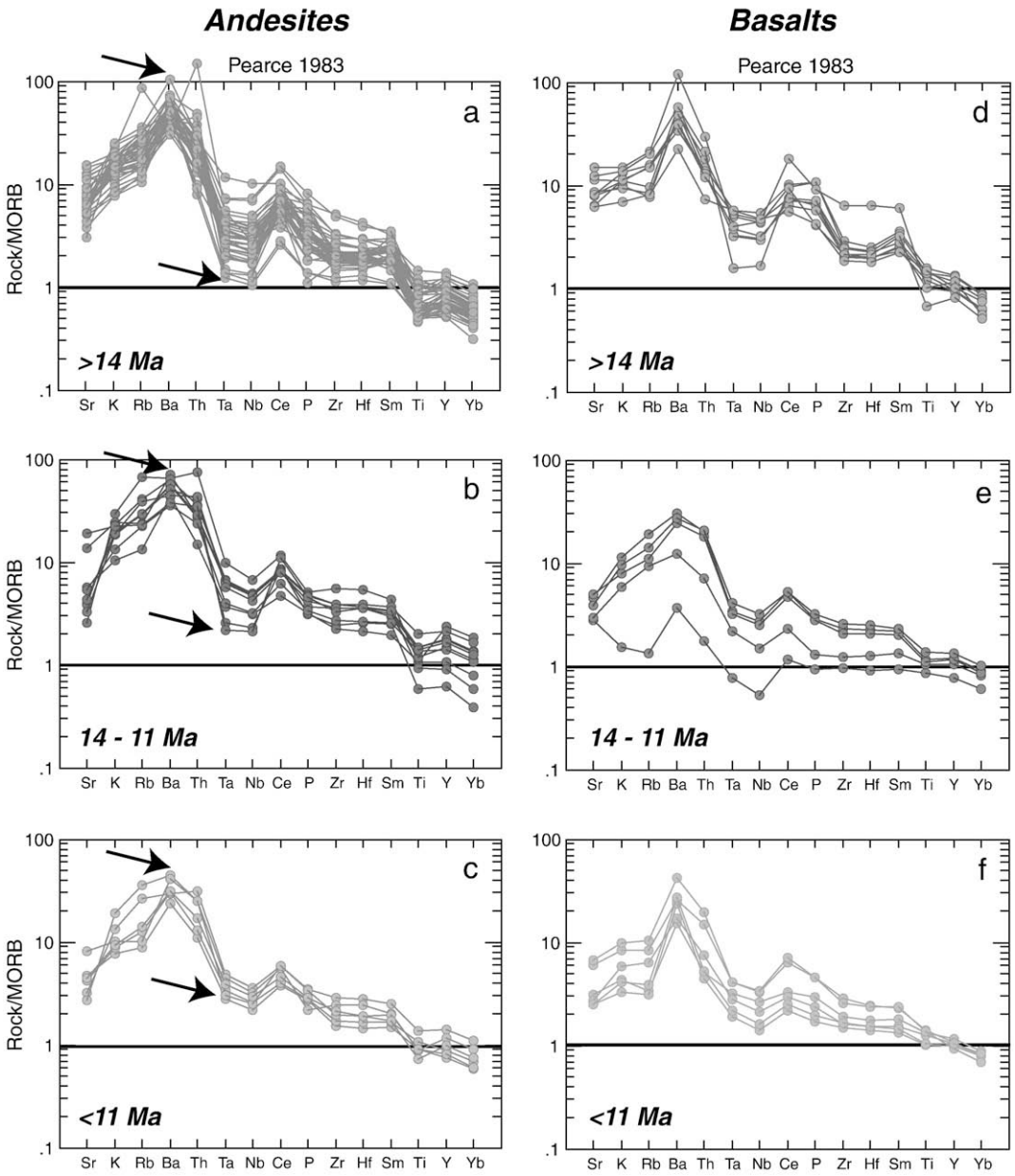

Fig. 3. MORB-normalized spider plots of all andesites (a–c) and basalts (d–f) with trace element analyses from Sonora. Plots are divided by sample age. Arrows on plots a–c illustrate the progressive waning of the HFSE depletion and LILE enrichment after subduction ceased.

Please cite this article as: Till, C.B., et al., Perils of petrotectonic modeling: A view from southern Sonora, Mexico, J. Volcanol. Geotherm. Res. (2009), doi:10.1016/j.jvolgeores.2009.06.014

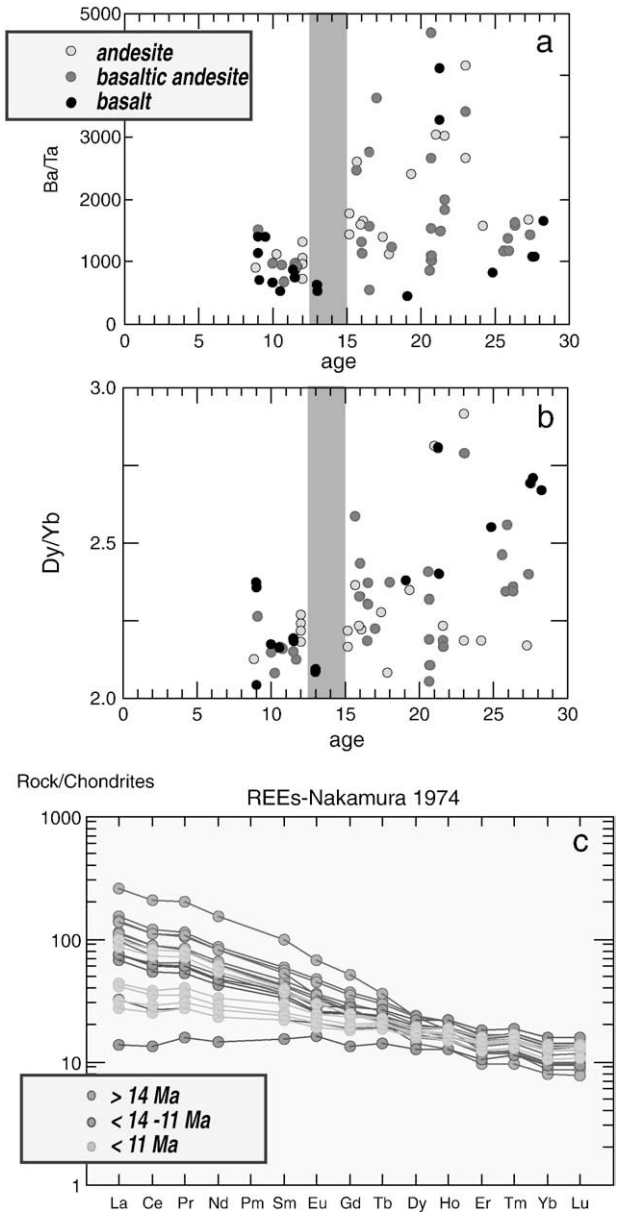

Fig. 4. Trace element ratios and REE plots for mafic samples from Sonora. Plots a. and b. are Ba/Ta and Dy/Yb ratios for all Sonoran andesites, basaltic andesites and basalts plotted against age. Gray box from 15–12.5 Ma denotes the approximate termination of subduction below Sonora. Plot c. is the REE concentration of all basalts color-coded by age.

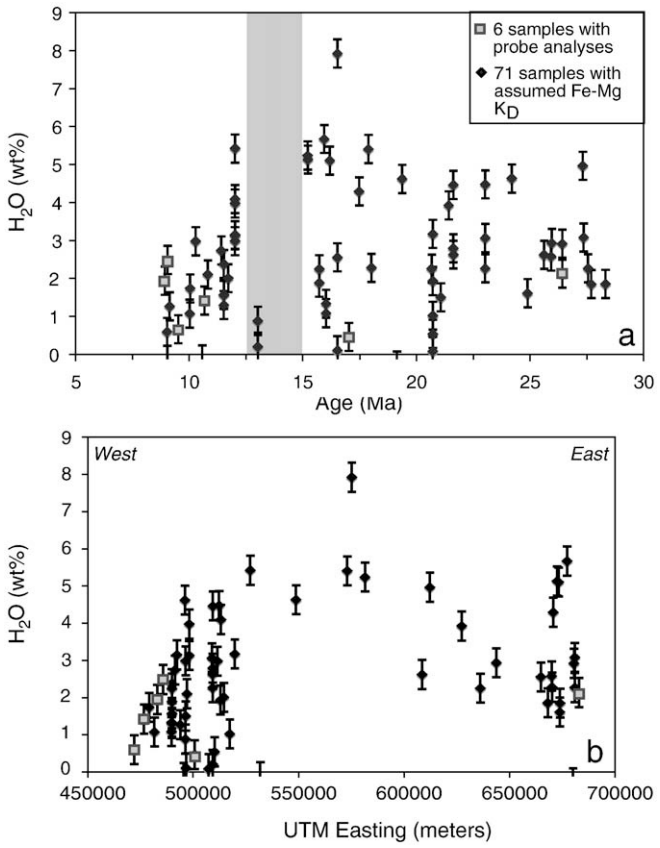

Fig. 5. Pre-eruptive H_2O-content for the 71 most mafic samples from Sonora plotted against time (a) and UTM easting (equivalent to longitude) (b). Pre-eruptive H_2O-content calculated using the olivine–clinopyroxene–plagioclase hydrometer of Sisson and Grove (1993). Square symbols denote subset of six samples for which H_2O-content was calculated using the phenocryst phase compositions rather than calculating the liquidus olivine composition, assuming a Fe–Mg K_D of 0.29. Average error is approximately 0.39 wt.% H_2O.

Similar to the Colorado River extensional corridor in the Basin and Range (Gans and Bohrson, 1998), the cessation of eruptive activity in Sonora at ~8 Ma may have been a thermobarometric consequence of extensional fracturing and thinning of the upper crust.

Our interpretation of conductive reheating causing post-subduction volcanism in Sonora is consistent with that of Castillo (2008), who proposes post-subduction volcanism in Baja was the result of influx of Pacific asthenosphere after the cessation of subduction, which provided the thermal energy to melt mafic lower crust to form adakites (Atherton and Petfrod, 1993; Negrete-Aranda and Cañón-Tapia, 2008) and the preexisting metasomatized mantle wedge, to produce bajaites and calc-alkaline magmas. Similarly, Vidal-Solano et al. (2008) conclude mid-Miocene volcanic rocks in Pinacate, Sonora, located northwest of our study area, formed during progressive thinning of the lithosphere and upwelling of asthenosphere, which they attribute to the formation of a slab window. As an alternative, Cañón-Tapia and Walker (2004) suggest there can be a sufficient lag time (on the order of ~10^6 years), between deep melt generation and surface eruption, to allow magma reservoirs to act as time capsules that record the prior tectonic setting. Mantle and crustal heterogeneities, as well as local stress fields, all likely effect when and where magma erupts. Thus, Negrete-Aranda and Cañón-Tapia (2008) suggest in Baja and in similar structurally-active tectonic settings, we should reject the assumption that magmas have short subsurface residence times and thus the hypothesis that the type of volcanic rocks erupted is coupled with the present tectonic setting.

The overall similarity in syn- and post-subduction mafic volcanic rocks erupted in southern Sonora suggest either they were produced by conductive reheating of subduction-modified mantle or by long crustal residence times. A time lag of $2.5–4\times10^6$ years, between formation and eruption, is required to explain the subduction character of most post-subduction magmas in southern Sonora, which is at the uppermost limit of residence times predicted by Cañón-Tapia and Walker (2004). Unlike the central and southern regions of the Baja peninsula, Sonora exhibits none of the traditional compositions of volcanism associated with extensional terrains, such as alkalic or tholeiitic basalt or bimodal rhyolitic and basaltic volcanism (Gastil et al., 1979; Hausback, 1984; Sawlan and Smith, 1984; Saunders et al., 1987; Bigioggero et al., 1995; Luhr et al., 1995). However, the presence of <12.5 Ma relatively anhydrous lavas in coastal Sonora suggest that not all post-subduction magmas acted as "time capsules" (Fig. 5b). Thus we favor a model where extension and asthenospheric upwelling caused melting of previously metasomatized mantle following subduction in southern Sonora, and recognize

Please cite this article as: Till, C.B., et al., Perils of petrotectonic modeling: A view from southern Sonora, Mexico, J. Volcanol. Geotherm. Res. (2009), doi:10.1016/j.jvolgeores.2009.06.014

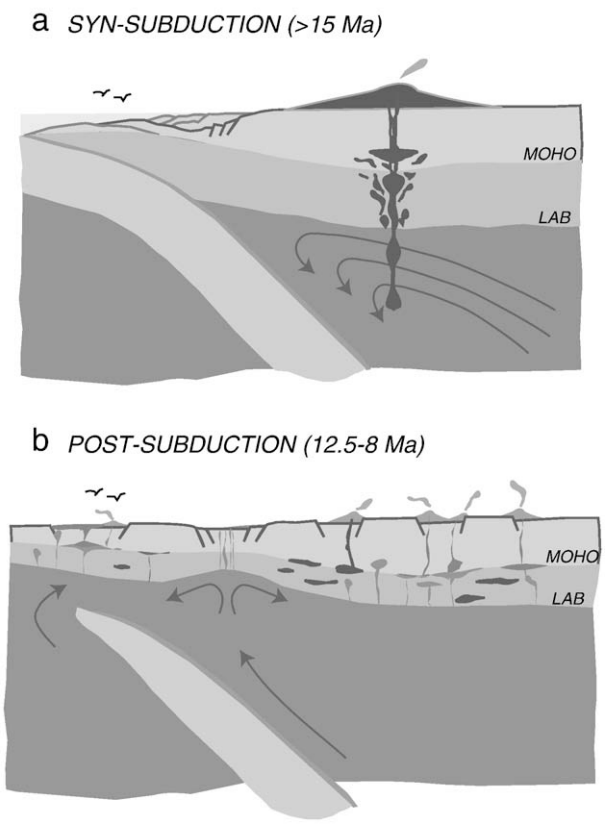

Fig. 6. Cartoon cross-section through the Gulf Extensional Province during subduction (a) and following the tectonic transition to oblique extension (b). Syn-subduction volcanism is the product of typical flux melting of hydrated mantle wedge peridotite. Post-subduction magmatism (<12.5 Ma) likely formed when proto-Gulf extension triggered conductive reheating and/or decompression melting of reservoirs of metasomatized mantle peridotite.

the potential that some magma reservoirs may have resided in the crust for on the order of 10^6 years before erupting.

6. Conclusion

The age-constrained major and trace element analyses presented in this study represent the most comprehensive geochemical database for Cenozoic volcanism in Sonora. Mafic volcanic rocks erupted in Sonora from 27 to 8 Ma have continental arc signatures and appear to be derived from the metasomatized sub-arc mantle below Sonora. Samples erupted during subduction (ca. 27–15 Ma) likely formed via typical flux melting of hydrated mantle wedge peridotite and subsequent fractionation processes in the crust. The residual arc trace element signatures and low pre-eruptive H_2O-content of samples erupted after subduction ceased (ca. 12.5–8 Ma) suggests the time required to completely erase the subduction signature from the sub-arc mantle was greater than the 4 million years of volcanism that post-dated subduction in Sonora. Post-subduction samples likely represent the remobilization of subduction-altered mantle lithosphere triggered by crustal extension in Sonora or had significant residence times in the crust. Southern Sonora is unlike central and southern regions of Baja, which demonstrate a change in the average composition of magmas erupted after subduction ceased ca. 11 Ma. Instead Sonora exhibits only subtle and protracted (>4 m.y.) changes in the geochemical record. Therefore although both Baja and Sonora experienced an abrupt (2.5 m.y.) change in tectonic setting, they exhibit very different responses in the geochemical record. This study demonstrates the need for caution for interpreting geochemical data in the absence of plate reconstructions.

Acknowledgements

This work was funded by the National Science Foundation. We thank J. Roldan-Quintana for logistical support, WSU GeoAnalytical Lab for analytical assistance, I. MacMillan for field support and C. Snow and B. Leeman for review comments on an earlier version of this paper.

Appendix A. Supplementary data

Supplementary data associated with this article can be found, in the online version, at doi:10.1016/j.jvolgeores.2009.06.014.

References

Aranda-Gomez, J.J., McDowell, F.W., 1998. Paleogene extension in the southern Basin and Range Province of Mexico; syndepositional tilting of Eocene red beds and Oligocene volcanic rocks in the Guanajuato mining district. International Geology Review 40 (2), 116–134.
Arculus, R.J., Johnson, R.W., 1981. Island-arc magma sources — a geochemical assessment of the roles of slab-derived components and crustal contamination. Geochemical Journal 15 (3), 109–133.
Atherton, M.P., Petford, N., 1993. Generation of sodium-rich-magmas from newly underplated basaltic crust. Nature 362, 144–146.
Atwater, T., 1970. Implications of plate tectonics for the Cenozoic tectonic evolution of western North America. Geological Society of America Bulletin 81 (12), 3513–3535.
Atwater, T., 1989. Plate tectonic history of the northeast Pacific and western North American. In: Winterer, E.L., et al. (Ed.), The Eastern Pacific Ocean and Hawaii: Geology of North America volume N. Geological Society of America, Boulder, Colorado, pp. 21–71.
Bigioggero, B., Chiesa, S., Zanchi, A., Montrasio, A., Vezzoli, L., 1995. The Cerro Mencenares volcanic center, Baja California Sur; source and tectonic control on postsubduction magmatism within the Gulf Rift. Geological Society of America Bulletin 107 (9), 1108–1122.
Blair, K.D., personal communication, 2006.
Blair, K., Gans, P.B., 2003. Stratigraphy of the Sahuaripa Basin and preliminary comparison to the Rio Yaqui Basin, east-central Sonora, Mexico. Abstracts with Programs-Geological Society of America 35 (4), 27.
Blair, K., Gans, P.B., 2005. The Sahuaripa Basin: episodic Cretaceous to Mid-Miocene extension and magmatism in the Northwestern Mexican Basin and Range. Abstracts with Programs-Geological Society of America 37 (7), 480.
Castillo, P.R., 2008. Origin of the adakite-high-Nb basalt association and its implications for postsubduction magmatism in Baja California, Mexico. Geological Society of America Bulletin 120 (3/4), 451–462.
Cañón-Tapia, E., Walker, G.P.L., 2004. Global aspects of volcanism: the perspectives of "plate tectonics" and "volcanic systems.". Earth Science Reviews 66, 163–182.
Chayes, F., 1964. A Petrographic distinction between Cenozoic Volcanics in and around the Open Oceans. Journal of Geophysical Research 69 (8), 1573–1588.
Christiansen, R.L., Lipman, P.W., 1972. Cenozoic Volcanism and Plate-Tectonic Evolution of the Western United States. II Late Cenozoic. Philosophical Transactions of the Royal Society of London. Series A, Mathematical and Physical Sciences 271 (1213), 249–284.
Daly, R.A., 1933. Igneous Rocks and the Depths of the Earth. McGraw-Hill, New York. 598 pp.
Dickinson, W.R., Snyder, W.S., 1979. Geometry of triple junctions related to San Andreas Transform. Journal of Geophysical Research 84 (NB2), 561–572.
Dupuy, C., Dostal, J., Marcelot, G., Bougault, H., Joron, J.L., Treuil, M., 1982. Geochemistry of basalts from Central and Southern New Hebrides Arc — implications for their source rock compositions. Earth and Planetary Science Letters 60 (2), 207–225.
Gans, P.B., 1997. Large-magnitude Oligo-Miocene extension in southern Sonora; implications for the tectonic evolution of Northwest Mexico. Tectonics 16 (3), 388–408.
Gans, P.B., personal communication, 2009.
Gans, P.B., Bohrson, W.A., 1998. Suppression of volcanism during rapid extension in the Basin and Range Province, United States. Science 279, 66–68.
Gans, P.B., Wong, M., MacMillan, I., Blair, K.D., Roldan, J., Till, C.B., Herman, S., 2006. Magmatic–tectonic interactions in the Gulf extensional province: insights from the Sonoran margin. Proceedings, MARGINS Workshop: Lithospheric Rupture in the Gulf of California — Salton Trough Region. http://www.rcl-cortez.wustl.edu/Presentations.html.
Gastil, R.G., Phillips, R.P., and Allison, E.C., 1975. Reconnaissance geology of the state of Baja California. Geological Society of America Memoir Map 140, scale 1; 250,000.
Gastil, G., Krummenacher, D., Minch, J., 1979. The record of Cenozoic volcanism around the Gulf of California. Geological Society of America Bulletin 90 (9), I839–I857.
Gastil, R.G., Neuhaus, J., Cassidy, M., Smith, J.T., Ingle Jr., J.C., Krummenacher, D., 1999. Geology and paleontology of southwestern Isla Tiburon, Sonora, Mexico. Revista Mexicana de Ciencias Geologicas 16 (1), 1–34.
Gill, J.B., 1981. Orogenic Andesites. Springer-Verlag, NewYork. 390 pp.

Please cite this article as: Till, C.B., et al., Perils of petrotectonic modeling: A view from southern Sonora, Mexico, J. Volcanol. Geotherm. Res. (2009), doi:10.1016/j.jvolgeores.2009.06.014

Grove, T.L., Parman, S.W., Bowring, S.A., Price, R.C., Baker, M.B., 2002. The role of an H_2O-rich fluid component in the generation of primitive basaltic andesites and andesites from the Mt. Shasta region, N California. Contributions to Mineralogy and Petrology 142, 375–396.

Hausback, B.P., 1984. Cenozoic volcanic and tectonic evolution of Baja California Sur, Mexico: Field Trip Guidebook — Pacific Section, Society of Economic Paleontologists and Mineralogists, vol. 39, pp. 219–236.

Herman, S.W., Gans, P.B., 2005. Large scale vertical axis rotations in coastal Sonora; evidence for transtensional proto-Gulf deformation. Abstracts with Programs-Geological Society of America 37 (7), 68.

Kelemen, P.B., Yogodzinski, G.M., Scholl, D.W., 2003. Along-strike variations in the Aleutian Island arc: genesis of high Mg# andesite and implications for continental crust. In: Eiler, J. (Ed.), Inside the Subduction Factory. American Geophysical Union, Washington DC, pp. 223–276.

Kovács, I., Szabó, C.S., 2008. Middle Miocene volcanism in the vicinity of the Middle Hungarian zone: evidence for an inherited enriched mantle source. Journal of Geodynamics 45, 1–17.

Le Bas, M.J., Le Maitre, R.W., Woolley, A.R., 1992. The construction of the total alkali-silica chemical classification of volcanic rocks. Mineralogy and Petrology 46, 1–22.

Lonsdale, P., 1991. Structural patterns of the Pacific floor offshore of Peninsular California. In: Dauphin, J.P., Simoneit, B.R.T. (Eds.), The Gulf and Peninsular Province of the Californias: AAPG Memoir, vol. 47, pp. 87–125.

Lonsdale, P., 2006. The opening of the Gulf of California Trough within the North American Cordillera. Abstracts with Programs — Geological Society of America Specialty Meeting, Backbone of the Americas, Mendoza, Argentina, p. 82.

Luhr, J.F., Aranda-Gomez, J.J., Housh, T.B., 1995. San Quintin volcanic field, Baja California Norte, Mexico: geology, petrology and geochemistry. Journal of Geophysical Research 100 (B7), 10353–10380.

MacMillan, I., personal communication, 2006.

MacMillan, I., Gans, P.B., Roldan, J., 2003. Voluminous mid-Miocene silicic volcanism and rapid extension in the Sierra Libre, Sonora, Mexico. Abstracts with Programs-Geological Society of America 35 (4), 26.

MacMillan, I., Gans, P.B., Till, C.B., 2005. Tectonic implications of the volcanic and structural history of the Sierra Santa Ursula, Sonora Mexico. Abstracts with Programs-Geological Society of America 37 (4), 64.

Marshall, P., 1912. Oceania, Handbuch der Regionalen Geologie, vol. 2. C. Winter, Heidelberg, pp. 1–36.

McDowell, F.W., Clabaugh, S.E., 1979. Ignimbrites of the Sierra Madre Occidental and their relation to the tectonic history of western Mexico. Special Paper-Geological Society of America 180, 113–124.

McDowell, F.W., Roldan Quintana, J., Amaya Martinez, R., 1997. Interrelationship of sedimentary and volcanic deposits associated with Tertiary extension in Sonora, Mexico. Geological Society of America Bulletin 109 (10), 1349–1360.

Mora-Klepeis, G., McDowell, F.W., 2004. Late Miocene calc-alkalic volcanism in northwestern Mexico: an expression of rift or subduction-related magmatism? Journal of South American Earth Sciences 17, 297–310.

Negrete-Aranda, R., Cañón-Tapia, E., 2008. Post-subduction volcanism in the Baja California Peninsula, Mexico: the effects of tectonic reconfiguration in volcanic systems. Lithos 102, 392–414.

Oskin, M., Stock, J., 2003. Cenozoic volcanism and tectonics of the continental margins of the upper Delfin Basin, northeastern Baja California and western Sonora. In: Johnson, S.E., et al. (Ed.), Tectonic Evolution of Northwestern Mexico and the Southwestern USA: Geological Society of America Special Paper, vol. 374, pp. 421–438. Boulder, Colorado.

Pearce, J.A., Cann, J.R., 1971. Ophiolite origin investigated by discriminant analysis using Ti, Zr and Y. Earth and Planetary Science Letters 12, 339.

Pearce, J.A., Cann, J.R., 1973. Tectonic setting of basic volcanic rocks determined using trace element analyses. Earth and Planetary Science Letters 19, 290–300.

Pearce, J.A., Peate, D.W., 1995. Tectonic implications of the composition of volcanic arc magmas. Annual Reviews of Earth and Planetary Sciences 23, 251–285.

Perfit, M.R., Gust, D.A., Bence, A.E., Arculus, R.J., Taylor, S.R., 1980. Chemical characteristics of island-arc basalts: implications for mantle sources. Chemical Geology 30, 227–256.

Saunders, A.D., Rogers, G., Marriner, G.F., Terrell, D.J., Verma, S.P, 1987. Geochemistry of Cenozoic volcanic rocks, Baja California, Mexico; implications for the petrogenesis of post-subduction magmas. Journal of Volcanology and Geothermal Research 32 (1–3), 223–245.

Sawlan, M.G., 1991. Magmatic evolution of the Gulf of California rift. In: Dauphin, J.P., Simoneit, B.R.T. (Eds.), The Gulf and Peninsular Province of the Californias: American Association of Petroleum Geologists Memoir, vol. 47, pp. 301–369. Tulsa, Oklahoma.

Sawlan, M.G., Smith, J.G., 1984. Late Cenozoic volcanic suites in northern Baja California Sur, Mexico; their relation to subduction and rifting along the Baja California Peninsula. Abstracts with Programs-Geological Society of America 16 (6), 645.

Sisson, T.W., Grove, T.L., 1993. Experimental investigations of the role of H_2O in calc-alkaline differentiation and subduction zone magmatism. Contributions to Mineralogy and Petrology 113 (2), 143–166.

Spera, F.J., Bohrson, W.A., Till, C.B., Ghiorso, M.S., 2007. Partitioning of trace elements among coexisting crystals, melt, and supercritical fluid during isobaric crystallization and melting. American Mineralogist 92 (11–12), 1881–1898.

Stock, J.M., Hodges, K.V., 1989. Pre-Pliocene extension around the Gulf of California, and the transfer of Baja California to the Pacific Plate. Tectonics 8 (1), 99–115.

Valencia-Moreno, M., Ruiz, J., Barton, M.D., Patchett, P.J., Zuercher, L., Hodkinson, D.J., Roldan-Quintana, J., 2001. A chemical and isotopic study of the Laramide granitic belt of northwestern Mexico; identification of the southern edge of the North American Precambrian basement. Geological Society of America Bulletin 113 (11), 1409–1422.

Vidal-Solano, J.R., Demant, A., Paz Moreno, F.A., Lapierre, H., Ortega-Rivera, M.A., Lee, J.K.W., 2008. Insights into the tectonomagmatic evolution of NW Mexico: geochronology and geochemistry of the Miocene volcanic rocks from the Pinacate area, Sonora. Geological Society of America Bulletin 120 (5/6), 691–708.

Weigand, P.W., Savage, K.L., Nicholson, C., 2002. The Conejo Volcanics and other Miocene volcanic suites in southwestern California. In: Barth, A. (Ed.), Contributions to Crustal Evolution of the Southwestern United States: Geological Society of America Special Paper, vol. 365, pp. 187–204. Boulder, Colorado.

Wong, M.S., Gans, P.B., 2003. Tectonic implications of early Miocene extensional unroofing of the Sierra Mazatán metamorphic core complex, Sonora, Mexico. Geology 31 (11), 953–956.

Wong, M.S., Gans, P.B., 2008. Geologic, structural, and thermochronologic constraints on the tectonic evolution of the Sierra Mazatan core complex, Sonora, Mexico: new insights into metamorphic core complex formation. Tectonics 27, 1–31.

Please cite this article as: Till, C.B., et al., Perils of petrotectonic modeling: A view from southern Sonora, Mexico, J. Volcanol. Geotherm. Res. (2009), doi:10.1016/j.jvolgeores.2009.06.014